STM JOURNALS

International Journal of
Molecular Biotechnological Research

Volume 1, Issue 1, 2023
January—June
DOI (Journal): 10.37591/IJMBR

https://journals.stmjournals.com/ijmbr/

Research IJMBR

In Silico Prediction of Multitarget Mechanism of Quinoline and Its Analogs on Phosphoinositide-3-Kinase Pathway Proteins

Nyaipriya Devi Sanglakpam*

Abstract

Objective: *Phosphoinositide 3-kinases (PI3Ks), the target of rapamycin (PI3K/Akt/mTOR, PAM), are a family of enzymes that play a role in the growth, proliferation, differentiation, motility, survival, and intracellular trafficking of cells, all of which are essential for healthy cellular function and are also connected to cancer. In this study, quinoline and its derivatives were employed to analyze its inhibition activity on the phosphoinositide-3-kinase pathway.* ***Methods:*** *In this work, eight phytocompounds from quinoline were chosen, and the phosphoinositide-3-kinase pathway was analyzed to assess their multitarget mechanism. The study was carried out computationally utilizing PubChem as a data source and the molecular structures of the phytocompounds, as well as Indian medicinal plants, phytochemistry, and treatments. For the pharmacological evaluation of these drugs under the ADME properties for toxicity prediction, several additional approaches were applied.* ***Results:*** *The docking data revealed that eight analogs of quinoline were the most potent inhibitors for the proteins, Akt PBD 3MV5, PDK1 3RWQ, PIK3 3S2A, and mTOR-4DRI.* ***Conclusion:*** *All these bioactive compounds could be regarded as worthy candidates for the inhibition of the phosphoinositide-3-kinase pathway due to their high affinity for the protein.*

Keywords: Phosphoinositide 3-kinase pathway, quinoline, 4DRI protein, 3MV5 protein, 3S2A protein, 3RWQ protein, multitarget mechanism

INTRODUCTION

Numerous essential cell functions, such as protein synthesis, cell proliferation, metabolism, survival, catabolism, and autophagy, depend on PI3K [1]. The phosphatidylinositol-3 kinase (PI3K) pathway, an essential intracellular signaling mechanism is altered or amplified in many malignancies, including breast, gastric, ovarian, colorectal, prostate, glioma, and endometrial cancer. Since the PI3K pathway is essential for cancer cell survival, angiogenesis, and metastasis, it is a promising therapeutic target [2]. Understanding the PI3K pathway's complexities may open new therapeutic paths because it is linked to several human disorders, including diabetes and cancer [1]. Many multifactorial and complicated diseases, including cancer, did not respond well to single site targeting because multiple sites may have needed to be addressed simultaneously. Moreover, several signaling pathways may hamper the effectiveness of single-target medications for treating complicated disorders. Finding a single agent that can operate on two or more targets simultaneously is the goal of multitarget therapies. Because the pharmacokinetics and pharmacodynamics of a single agent targeted to several protein molecules

***Author for Correspondence**
Nyaipriya Devi Sanglakpam
E-mail: nyaipriyas@gmail.com

Student, Department of Biotechnology, Ramaiah University of Applied Sciences, Mathikere, Karnataka, India

Received Date: March 02, 2023
Accepted Date: March 12, 2023
Published Date: April 20, 2023

Citation: Nyaipriya Devi Sanglakpam. In Silico Prediction of Multitarget Mechanism of Quinoline and Its Analogues on Phosphoinositide-3-Kinase Pathway Proteins. International Journal of Molecular Biotechnological and Research. 2023;1(1): 57–76p.

are more predictable than those of concurrent use of two or more single-targeted agents, it is assumed that this technique is pharmacologically more significant and may be predicted [3]. As mentioned earlier, the PI3K signaling pathway involves a cascade of protein molecules that control a variety of cellular functions [1]. The PI3K pathway is one of the most often activated signal transduction pathways in human prostate cancer and is important for cellular development and metabolism [4, 3].

Quinoline is an aromatic heterocyclic organic molecule with the chemical formula C9H7N. Quinoline's double-ring structure is created by the fusion of the benzene ring with pyridine at two nearby carbon atoms. Quinoline is an anticancer drug as its analogs have demonstrated significant effects through a variety of mechanisms, including growth regulators through apoptosis, disruption of cell migration, inhibition of angiogenesis, regulation of nuclear receptor responsiveness, and cell cycle arrest, etc. The efficacy of quinoline derivatives has been demonstrated in several cancer cell lines, including those for breast, colon, lung, colorectal, renal, etc. [5].

Quinoline serves as a recognized blueprint for creating PI3K/mTOR dual inhibitors [6, 7]. Numerous quinoline analogs, synthesized or derived from natural sources, are crucial for medicinal chemistry and biological usage. The growing interest in the development of anticancer medications is being shown for quinoline compounds that intercalate DNA. There are various research initiatives aimed at creating novel methods for a range of heterocyclic ring systems for anticancer activities, particularly those including 3-quinoline derivatives [8].

METHODOLOGY

Retrieval of Ligands

50 ligands were searched at IMPPAT a curated database of Indian Medicinal Plants, Phytochemistry, and Therapeutics (*https://cb.imsc.res.in/imppat/home*) [9]**.** The Canonical SMILES of all the ligands selected for the current experiment were recorded. The top eight ligands were retrieved from PubChem in SDF format (*https://pubchem. ncbi.nlm.nih.gov/*) [10].

Protein Retrieval

Proteins Akt PBD 3MV5, PDKI 3RWQ, PIK3 32SA, and Mtor-4DRI with PDB ID 3MV5, 3RWQ, 32SA, and 4DRI respectively were retrieved from RCSB PDB databank, which distributes structural factor files, NMR constraint files, and coordinate data. It also offers documentation and derived data (*https://www.rcsb.org/*) [11]. They proceeded for purification. The protein is downloaded in the PDB format (Figures 1–4). The resolution of the proteins downloaded are 2.47Å, 2.55Å, 2.55Å and 1.45Å, respectively. The method of retrieval of the protein is X-ray diffraction.

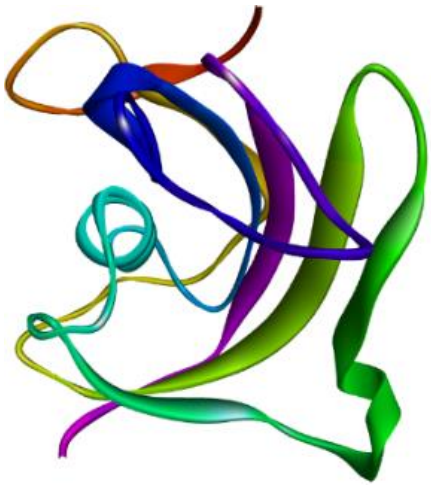

Figure 1. Structure of 4DRI.

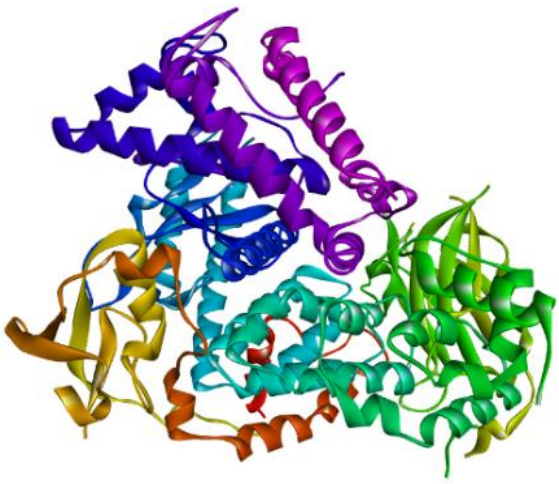

Figure 2. Structure of 3S2A.

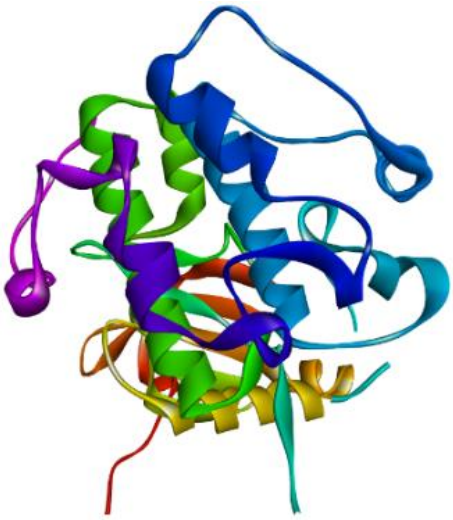

Figure 3. Structure of 3RWQ.

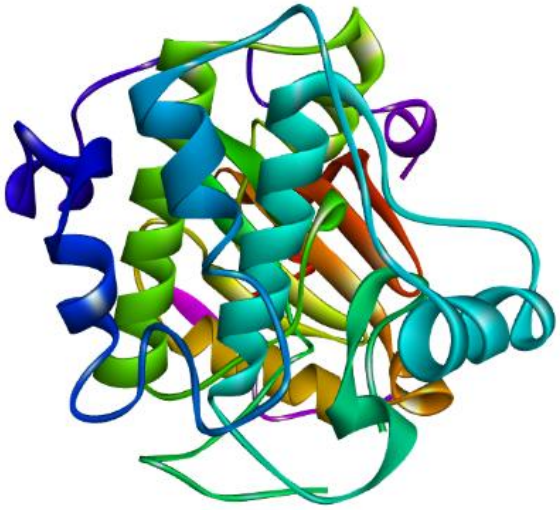

Figure 4. Structure of 3MV5.

Purification of Proteins

The proteins 3RWQ, 4DRI, 3MV5, and 3S2A have been purified in BIOVIA Discovery Studio 2021 Client, a molecular modeling application with several features for viewing, sharing, and analyzing data on proteins and small molecules [12]. Input protein molecules were created, and alterations were made to the raw PDB structure by assigning polar hydrogen atoms and removing ligand groups and hetero atoms. Water molecules were eliminated before docking because they can affect docking scores. Chain A was left intact for analysis while other chains were removed from the protein structures to make them simpler. Polar hydrogen atoms are introduced to purified structures to enhance their quality. To accelerate ligand binding chosen for the analysis, the prebound ligands are removed from the crystal structures.

Protein Structure Validation

Ramachandran plot for the purified proteins was constructed in PDBsum, a database that details the information of every 3D macromolecular structure stored in the Protein Data Bank (*http://www.ebi.ac.uk/thornton-srv/databases/pdbsum/Generate.html*) [13]. Additionally, a hydrophobicity map was generated from BIOVIA Discovery Studio [12]. To determine the secondary structures, PDBsum was used.

Molecular Docking

Using PyRx, a virtual screening tool for computational drug discovery that can be used to assess libraries of compounds against potential drug targets, molecular docking studies with the chosen ligand molecules and purified proteins were carried out (*https://pyrx.sourceforge.io/*) [14]. The study included 20 ligands of quinoline and its analogs and four proteins. Each of these compounds was docked into four different target protein molecules 3RWQ, 4DRI, 3MV5, and 3S2A and the docking conformation possessing the lowest energy was selected.

Physiochemical Studies (ADMET Screening)

By assessing characteristics such as physiochemical properties, medicinal chemistry, absorption, distribution, and toxicity, the ADMET analysis speeds up the drug discovery process. To uncover drug similarity characteristics and assess pharmacological efficacy as a potential candidate for drug development, ADMET properties are necessary. Using ADMETlab 2.0, a web server that provides the precise attribute values for the pharmaceuticals, ADMET analysis was carried out (*https://admetmesh.scbdd.com/*) [15]. The ligands with the highest binding affinities were chosen for ADMET analysis based on the docking data, and the Canonical SMILES were obtained from PubChem and evaluated using ADMET in ADMETlab 2.0.

Visualization

The top 5 ligand structures with the best binding score were then selected and then downloaded in PDB format after which they were visualized in BIOVIA Discovery Visualizer and the 2D, and 3D models were obtained [12].

RESULTS

For each protein, the top 5 ligands with the best binding were visualized. Following the docking research, it was discovered that eight of the ligands were common which inhibited the protein.

Protein Structure Analysis

Secondary Structure

To analyze the secondary structure of 4DRI, 3S2A, 3RWQ, and 3MV5, PDBsum was utilized. This tool displays the molecules that make up the 3D structure as well as their schematic interactions. As per the data obtained in Figure 5e, the secondary structure of 4DRI has 1 sheet, 3 beta hairpins, 6 beta bulges, 7 strands, 3 helices, and 13 beta turns. The structure has a total of 121 residues. 3S2A has 6 sheets, 10 beta hairpins, 10 beta bulges, 26 strands, 41 helices, and 38 beta turns. The structure has a total of 834 residues (Figure 6e). 3RWQ has 3 sheets, 4 beta hairpins, 5 beta bulges, 9 strands, 15 helices, and 19 beta turns. The structure has a total of 283 residues (Figure 7e). 3MV5 has 2 sheets, 4 beta hairpins, 5 beta bulges, 8 strands, 15 helices, and 23 beta turns. The structure has a total of 315 residues (Figure 8e).

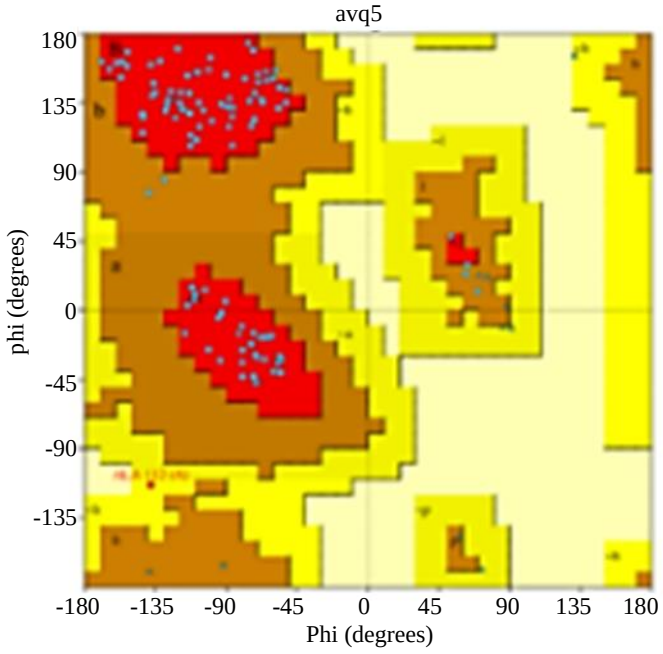

(a)

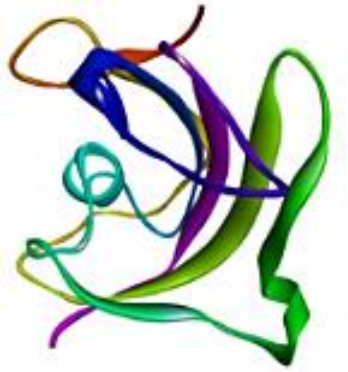

(b)

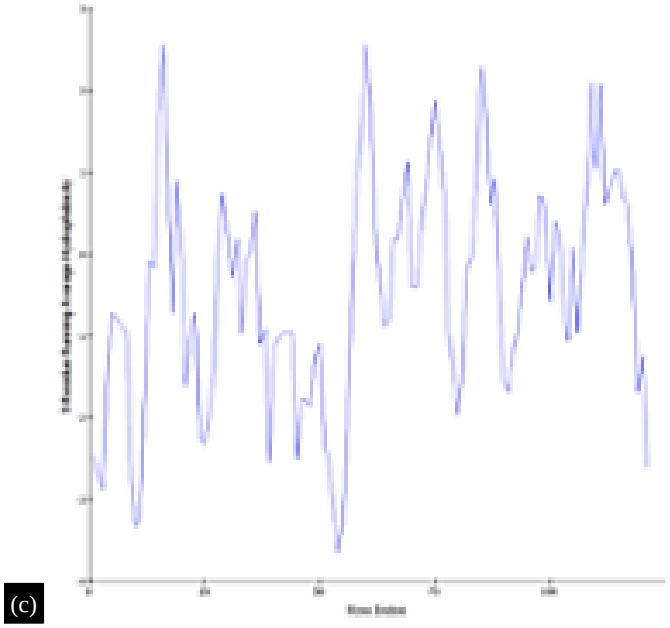

(c)

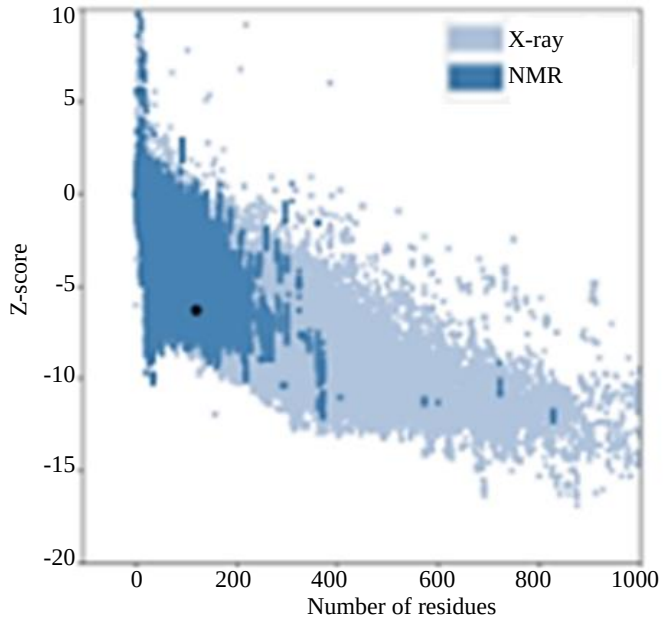

(d)

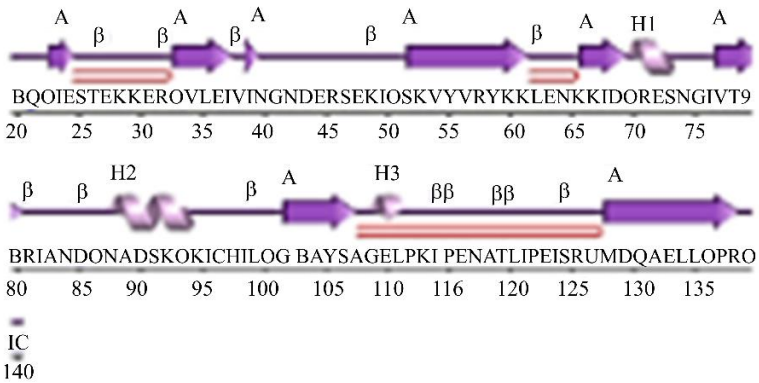

(e)

Figure 5. 4DRI. (a) Ramachandran plot, (b) 3D model, (c) hydrophobicity plot, (d) overall model quality, (e) secondary structure.

Ramachandran Plot

The Ramachandran plot helps to visualize the energetically permissible regions for the amino acid torsions angle ψ against φ in a protein structure. To create the Ramachandran plot of 4DRI, 3S2A, 3RWQ, and 3MV5, BIOVIA was employed as shown in Figures 5–8. On the graph, the red areas are the sterically permissible areas where peptide structure is stable. More than 88% of the amino acids must be in the sterically permissible zone for *in silico* analyses.

In protein 4DRI, about 93 residues of the amino acid residues fell in the most favored region, none in the disallowed region. Out of the 121 residues, 14 were glycine residues, 5 proline residues, 2 end residues, and 100 non-proline and non-glycine residues (Figure 5a). In 3S2A, about 665 residues of the amino acid residues fell in the most favored region, none in the disallowed region. Out of the 834 residues, 36 were glycine residues, 35 were proline residues, 19 were end residues, and 744 were non-proline and non-glycine residues (Figure 6a). 3RWQ had about 221 residues of the amino acid residues in the most favored region, whereas 1 residue was in the disallowed region. Out of the 283 residues, 16 were glycine residues, 16 were proline residues, 4 were end residues, and 247 were non-proline and non-glycine residues (Figure 7a). 3MV5 had about 247 residues of the amino acid residues fall in the most favored region, whereas 1 residue fell in the disallowed region. Out of the 315 residues, 22 were glycine residues, 12 proline residues, 6 end residues, and 275 non-proline and non-glycine residues (Figure 8a).

Overall Model Quality

For the overall model quality, ProSA (*https://prosa.services.came.sbg.ac.at/prosa.php*) was utilized. After the analysis, it was found that 4DRI had a Z-Score of -6.25 (Figure 5d). 3S2A had a Z-Score of -11.42 (Figure 6d). 3RWQ had a Z-Score of -7.05 (Figure 7d). 3MV5 had a Z-Score of -7.17 (Figure 8d).

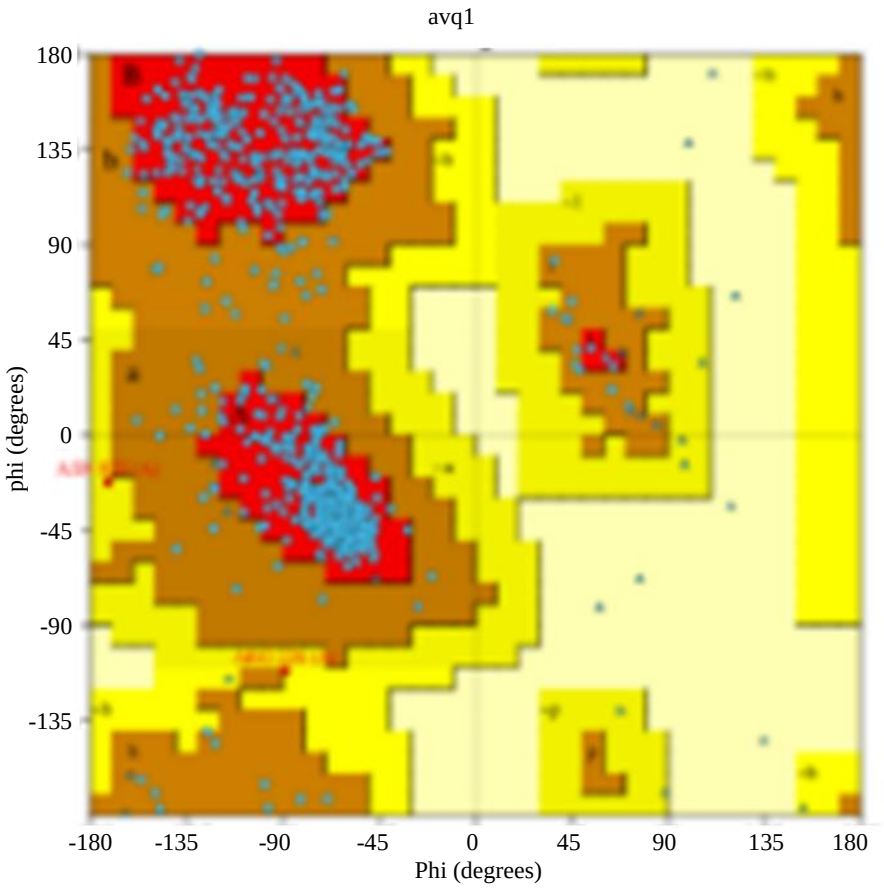

(a)

(b)

(c)

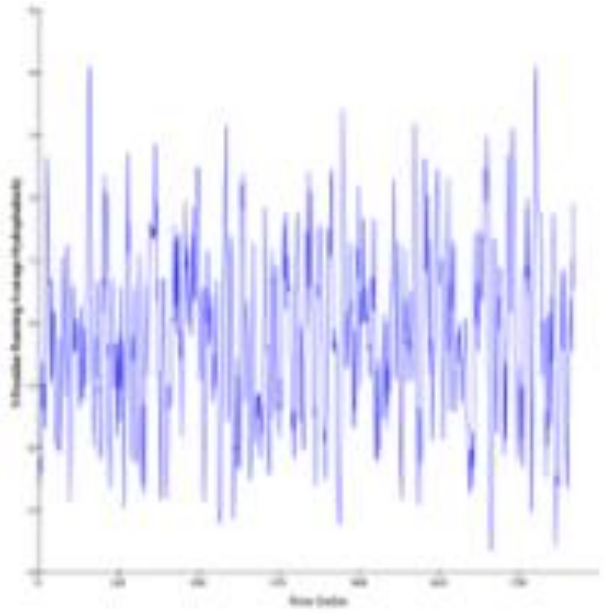

(d)

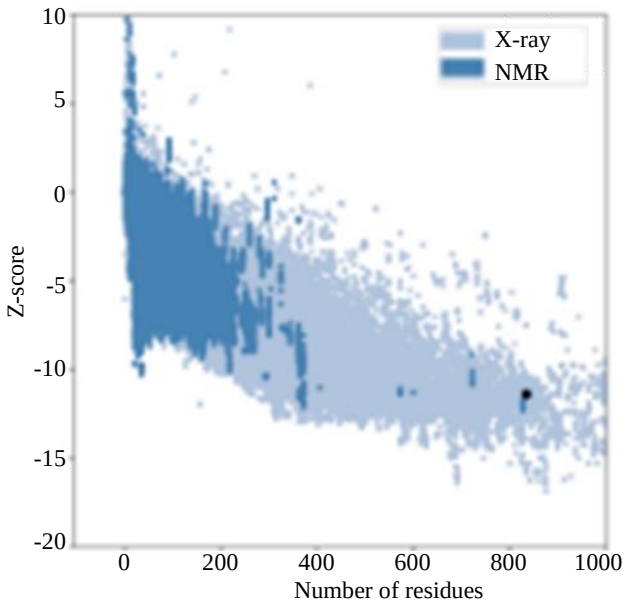

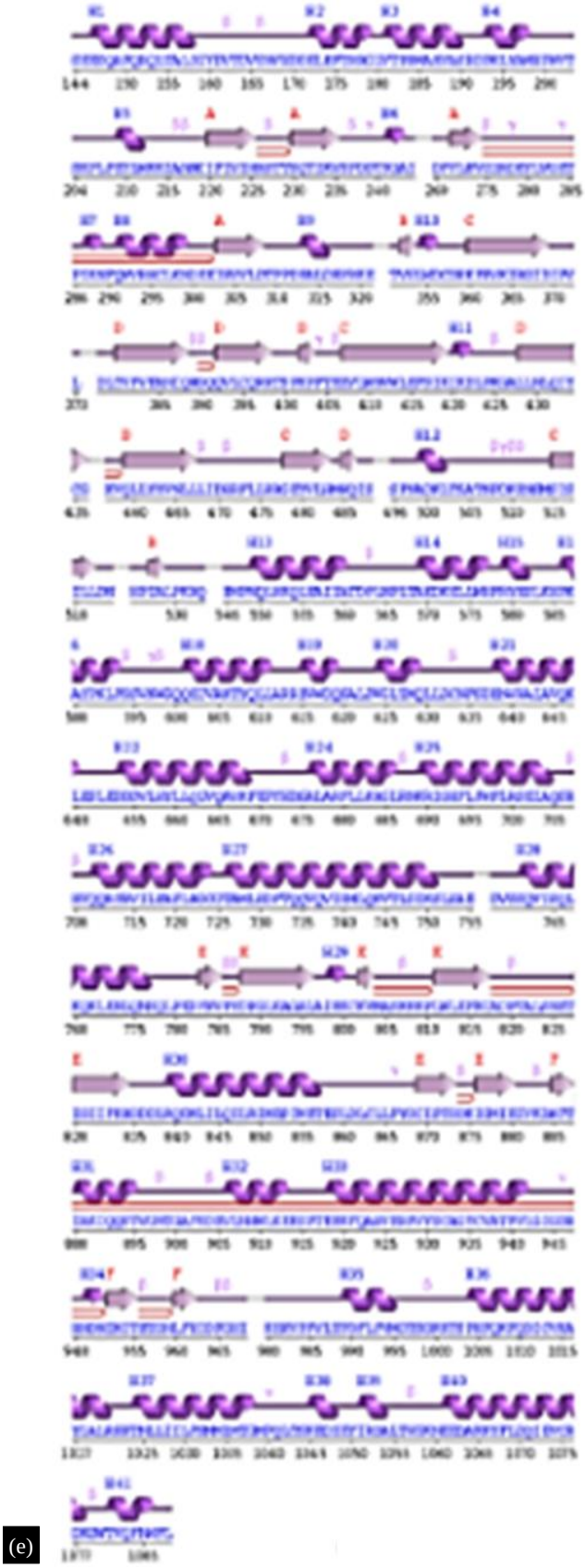

(e)

Figure 6. 3S2A (a) Ramachandran plot: (b) 3D model, (c) hydrophobicity plot, (d) overall model quality, (e) secondary structure.

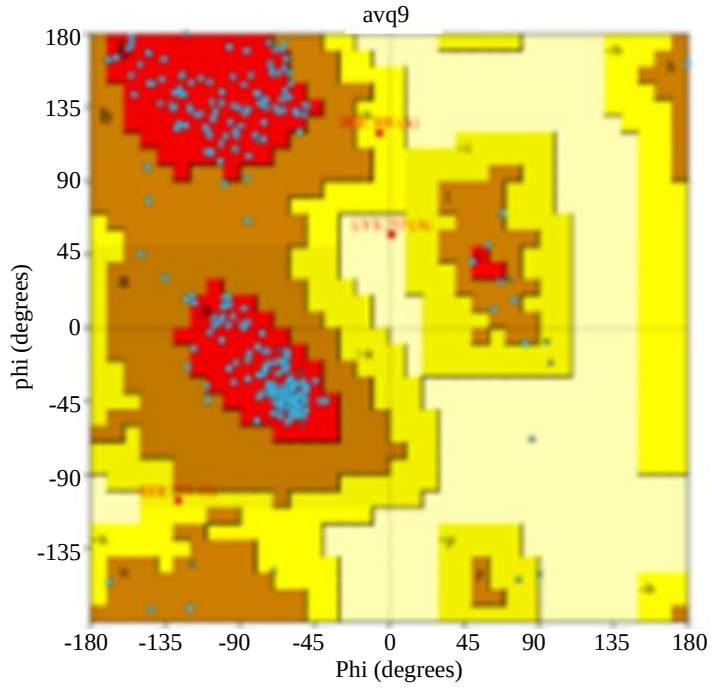

(a)

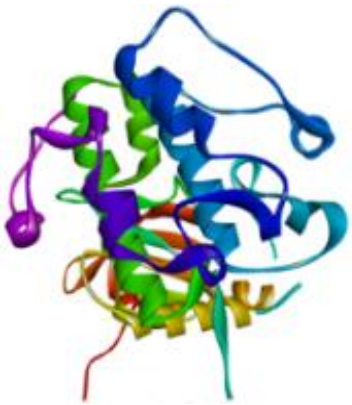

(b)

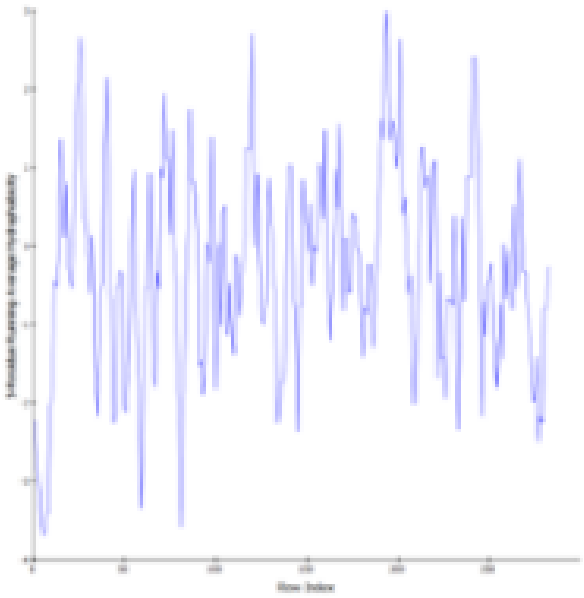

(c)

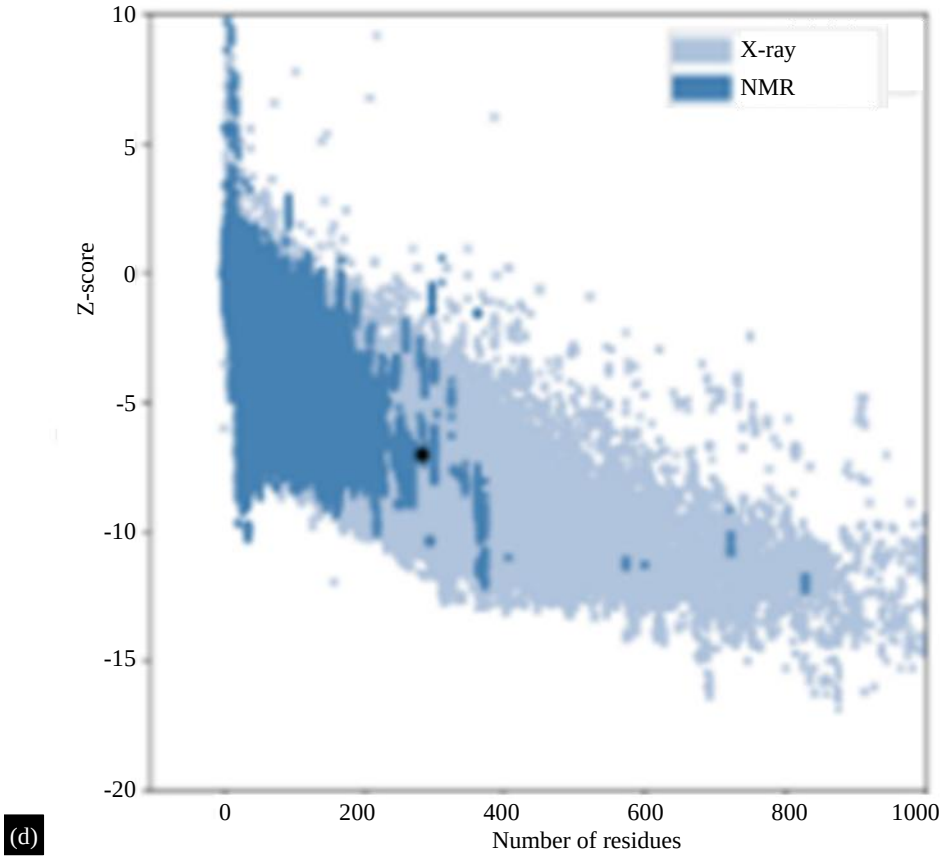

(d)

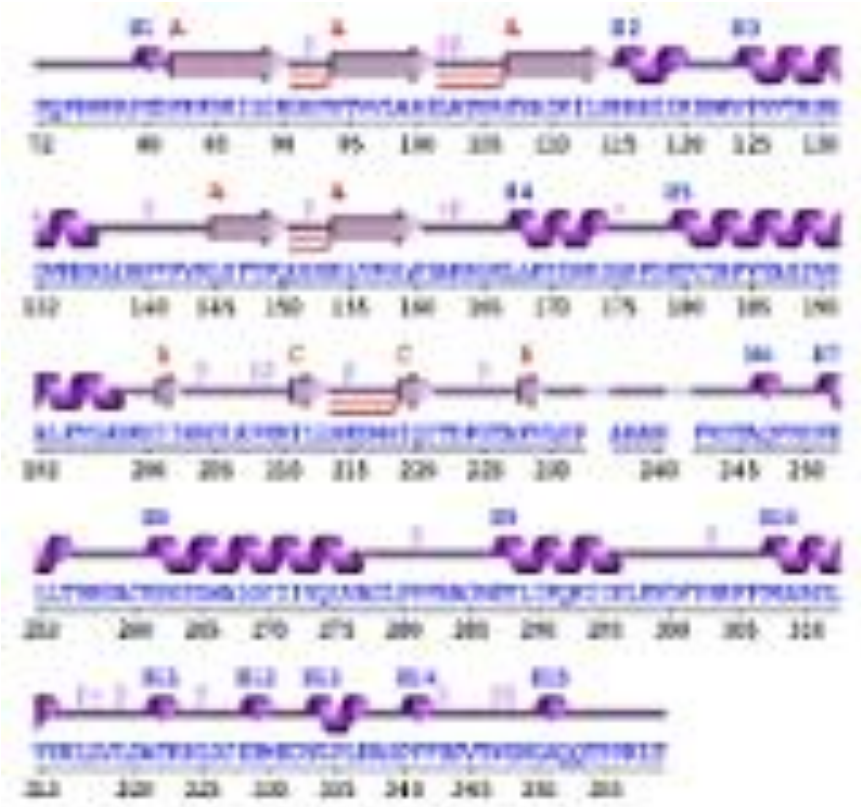

(e)

Figure 7. 3RWQ: (a) Ramachandran plot, (b) 3D model, (c) hydrophobicity plot, (d) overall model quality, (e) secondary structure.

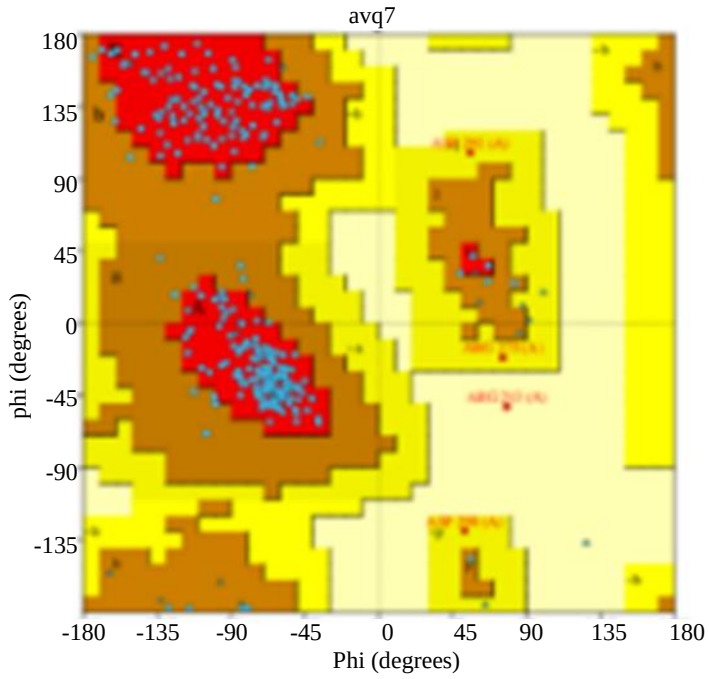

(a)

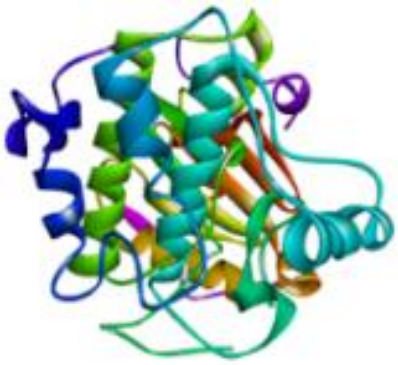

(b)

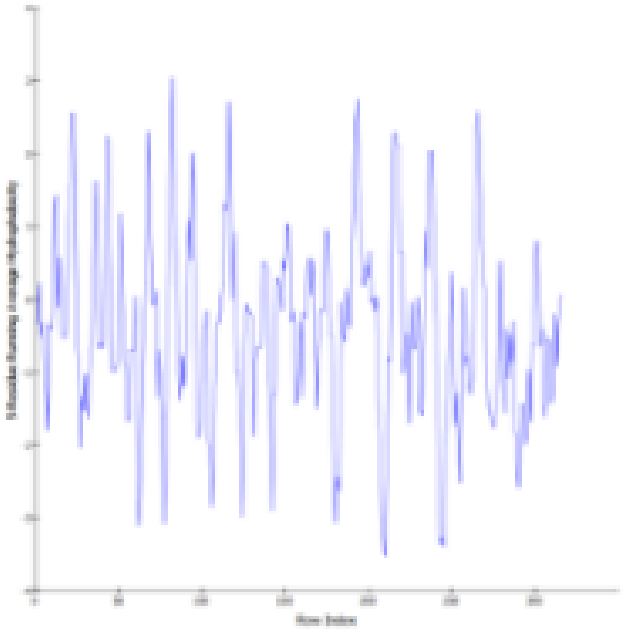

(c)

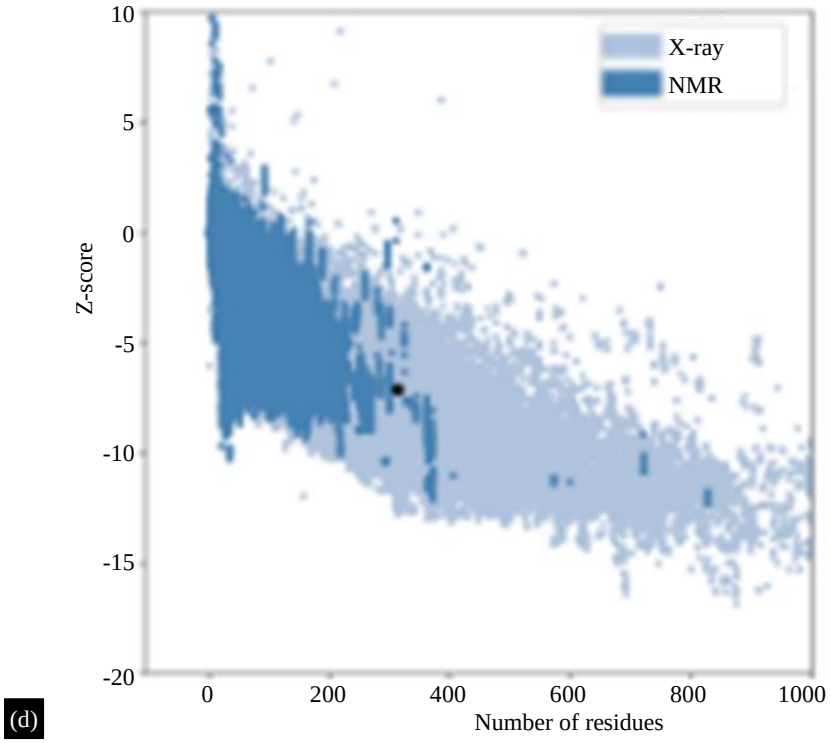

(d)

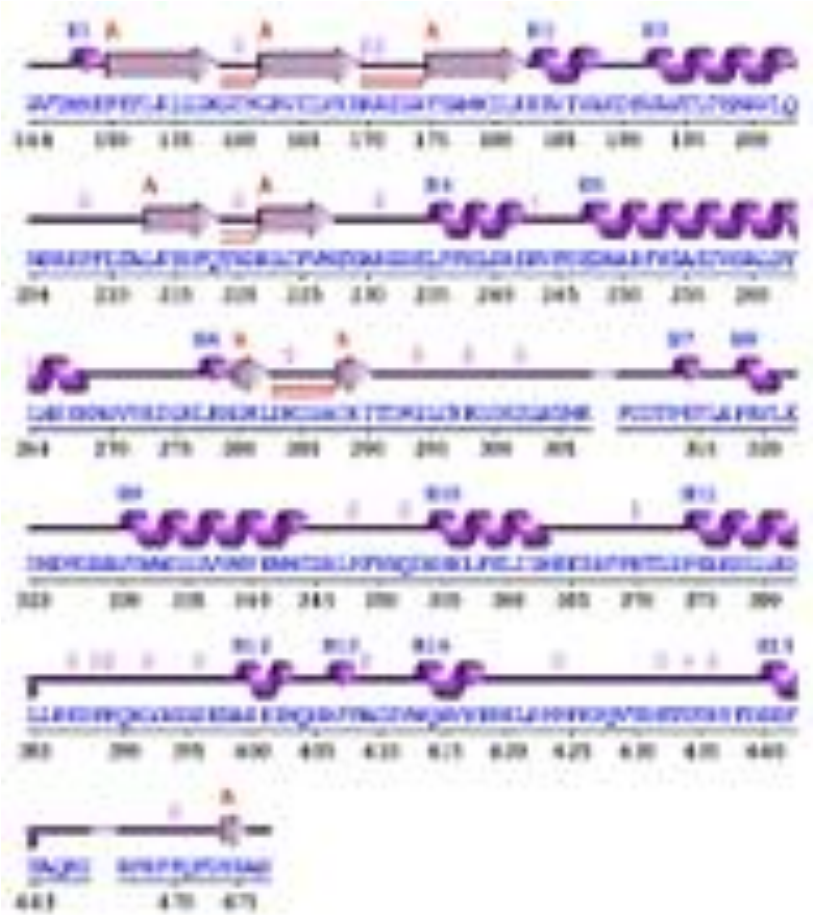

(e)

Figure 8. 3MV5: (a) Ramachandran plot, (b) 3D model, (c) hydrophobicity plot, (d) overall model quality, (e) secondary structure.

ADMET Analysis

Physiochemical properties

All the ligands fall under the optimal molecular weight as they are between 100 and 600. The ligands have the optimal number of hydrogen bond acceptors as they fall between 0 and 12 and have an optimal number of hydrogen bond donors. The ligands had an optimal number of rotatable bonds as they fall between 0 and 11 based on the Drug-Like Soft rule. All the ligands except ligand 156697 have an optimal number of rotatable bonds as they fall between 0 and 6 based on the Drug-Like Soft rule. 156697 had a value of nRing 7. All the ligands except ligand 11066 have an optimal number of atoms in the biggest ring as they fall between 0 and 18 based on the Drug-Like Soft rule. 11066 had a value of MaxRing 21. All the ligands have an optimal number of heteroatoms as they fall between 0 and 15 based on the Drug-Like Soft rule. All the ligands except 156697 have an optimal number of rigid bonds as they fall between 0 and 30 while 156697 had a value of nRig 37. Additionally, the ligands have an optimal number of Topological Polar Surface Areas as they fall between 0 and 140 based on the Veber rule. The results for the physiochemical properties of the top ligands are documented in Table 1.

Medicinal Chemistry Properties

The ligands 11066, 155514, and 157218 have the most attractive quality as per QED analysis. Whereas all ligands except 22169421, 25218881, and 156697 fall under the Lipinski rule as the logP value is more than 5 and the latter has an MW of more than 500. Ligands 457732 and 155514 have PAINS alert 1 which means all the ligands except these two do not cause off-target binding. All the ligands have low sp3 hybridized carbons/total carbon count and appreciable SASCORE which makes them a favorable drug candidate. The results for the medicinal chemistry properties of the top ligands are documented in Table 2.

Distribution Properties

All the ligands fall under the BBB+ category since logBB>-1, which interprets that there are very few side effects in the CNS since minimal or no BBB penetration is necessary to prevent CNS side effects. BBB must be crossed for medications to reach their molecular targets in the CNS. Ligand 25218881 has the least side effects with BBB penetration of 0.068. In the context of the predicted value of <90% which indicates strong protein binding, 157218 possesses the most appropriate PPB and thus binds with a high degree. All the ligands have proper VD since their predicted value falls under the range of 0.04-20L/k. 157218 has the highest Fu since it has the highest value of 15.82%. The results for the distribution properties of the top ligands are documented in Table 3.

Absorption Properties

All ligands except 156697 have proper Cao-2 permeability as it has a predicted value >-5.15 log cm/s. 25218881 has the highest PGP inhibitor with a value of 0.009. The ligand 457732 falls under category 0 while others fall in category 1. Out of the 25218881 has the highest PGP substrate. 11066 and 25218881 have the least human intestinal absorption with a value of 0.002. The ligand 25218881 had the most efficient F20% delivery while 25218881 and 11066 had the most efficient F30**%** delivery. The results for the absorption properties of the top ligands are documented in Table 4.

Toxicity Properties

All the ligands fall under the hERG+ category since the IGC50 value was less than 10 μM. All the ligands fall under DILI category 1. Ligand 157218 was found to be the most toxic since it had a value of 0.141. The ligand 157218 falls under the most toxic area while 156697, 11066, and 155514 are less toxic, and 22169421, 457732, and 23345 are the least toxic. The ligand 157218 was predicted to be the most toxic as per AMES evaluation and 23345 as per FDAMDD evaluation. The carcinogenicity prediction appraised 156697 as the most toxic. Table 5 shows the toxicity standard assessment.

Molecular Docking

For statistical evaluation, the docking conformation that had the highest binding energy was taken into consideration. In proteins 4DRI, 3S2A, 3MV5, and 3RWQ among the 50 ligands screened, the

phytocompounds having binding affinity above -7 towards each target protein were chosen in this analysis; thus, the compounds given in the tables (Tables 6–9) correspond to that category. The five ligands from each protein were therefore picked for additional analysis.

Table 1. Physicochemical properties of the ligand molecules.

ID	MW	nHA	nHD	nRot	nRing	MaxRing	nHet	nRig	Flex	TPSA	LogS	LogD	LogP
156697	608.29	8	2	7	7	16	8	37	0.189	83.86	-3.564	3.854	4.857
11066	351.11	6	0	2	5	21	6	26	0.077	58.92	-5.524	3.432	3.575
22169421	309.15	1	0	4	4	10	1	23	0.174	12.89	-6.401	4.458	5.558
155514	327.15	5	2	2	4	16	5	20	0.1	62.16	-1.667	2.452	2.243
25218881	339.07	4	0	2	4	10	5	22	0.091	48.42	-7.007	4.043	5.088
457732	223.06	3	0	0	3	14	3	18	0	47.03	-4.82	2.344	2.788
23345	219.1	1	0	2	3	10	1	17	0.118	12.89	-4.465	3.643	3.926
157218	343.18	5	1	6	3	10	5	17	0.353	48.95	-2.253	3.005	2.498

Table 2. Medicinal properties of the ligand molecules.

ID	QED	PAINS	Lipinski	Fsp3	SASCORE
156697	0.248	0	Accepted	0.351	3.835
11066	0.71	0	Accepted	0.25	2.573
22169421	0.491	0	Accepted	0.087	1.89
155514	0.831	1	Accepted	0.368	3.068
25218881	0.639	0	Accepted	0.158	2.319
457732	0.586	1	Accepted	0.071	2.059
23345	0.638	0	Accepted	0.062	1.635
157218	0.873	0	Accepted	0.4	2.756

Table 3. Distribution properties of the ligand molecules.

ID	BBB	PPB	VDss	Fu
156697	0.384	95.39%	1.282	5.51%
11066	0.357	93.51%	0.652	2.08%
22169421	0.495	99.43%	0.898	1.10%
155514	0.929	90.95%	1.613	10.91%
25218881	0.068	99.95%	0.506	0.93%
457732	0.331	94.98%	1.148	2.81%
23345	0.84	96.38%	2.041	2.90%
157218	0.903	69.41%	1.909	15.82%

Table 4. Absorption value of the ligand molecules.

ID	Caco-2	MDCK	Pgp-inh	Pgp-sub	HIA	F(20%)	F (30%)
156697	-5.593	1.58E-05	0.996	0.02	0.008	0.027	0.926
11066	-4.939	3.81E-05	0.132	0.002	0.002	0.005	0.005
22169421	-4.916	2.82E-05	0.903	0.669	0.007	0.999	0.133
155514	-4.815	1.14E-05	0.016	0.279	0.013	0.042	0.056
25218881	-4.835	2.32E-05	0.009	0.001	0.002	0.002	0.005
457732	-4.715	1.75E-05	0.096	0	0.005	0.003	0.801
23345	-4.573	3.18E-05	0.092	0.207	0.007	0.996	0.137
157218	-4.84	1.65E-05	0.976	0.891	0.003	0.004	0.033

Table 5. Toxicity standard assessment.

ID	hERG	DILI	AMES	FDAMDD	Carcinogenicity	IGC50	LC50
156697	0.944	0.426	0.131	0.946	0.028	5.229	7.632
11066	0.104	0.67	0.855	0.909	0.953	4.465	5.989
22169421	0.39	0.922	0.735	0.726	0.689	4.967	5.946
155514	0.427	0.475	0.429	0.914	0.036	4.634	5.534
25218881	0.078	0.738	0.88	0.833	0.92	4.934	5.849
457732	0.035	0.944	0.938	0.749	0.927	5.084	5.042
23345	0.108	0.949	0.746	0.153	0.629	4.109	4.645
157218	0.854	0.141	0.064	0.895	0.034	3.879	5.201

Table 6. Docking score of 4DRI protein with selected ligands.

Ligand	Binding Affinity
22169421	-8.7
156697	-8
23345	-7.9
25218881	-7.7
457732	-7.7

Table 7. Docking score of 3S2A protein with selected ligands.

Ligand	Binding Affinity
11066	-8.3
457732	-8.2
23345	-7.8
22169421	-7.3
157218	-7.2

Table 8. Docking score of 3RWQ protein with selected ligands.

Ligand	Binding Affinity
156697	-11.2
11066	-9.4
22169421	-9.4
155514	-9
25218881	-8.8

Table 9. Docking score of 3MV5 protein with selected ligands.

Ligand	Binding Affinity
22169421	-8.8
25218881	-8.8
156697	-8.7
11066	-8.3
457732	-8

Visualization

In protein 3MV5, Pi-sigma, Pi-alkyl, and alkyl bonds were observed while binding with 25218881. Pi-Sigma, Pi-Pi T-shaped, Pi-Pi Stacked, and Pi-alkyl were observed while binding with 22169421. Pi-anion, Pi-alkyl, and Pi-sigma were observed with 457732. Van der Waals, Pi-sigma, Pi-anion, alkyl, and Pi-alkyl were observed while binding with 156697. While binding with 11066, Pi-anion, Pi-cation, and Pi-Pi T-shape were observed (Figure 9, Figures 10–12 shows 2D interaction of molecular interactions of 3RWQ and 3MV5 with the ligands, respectively).

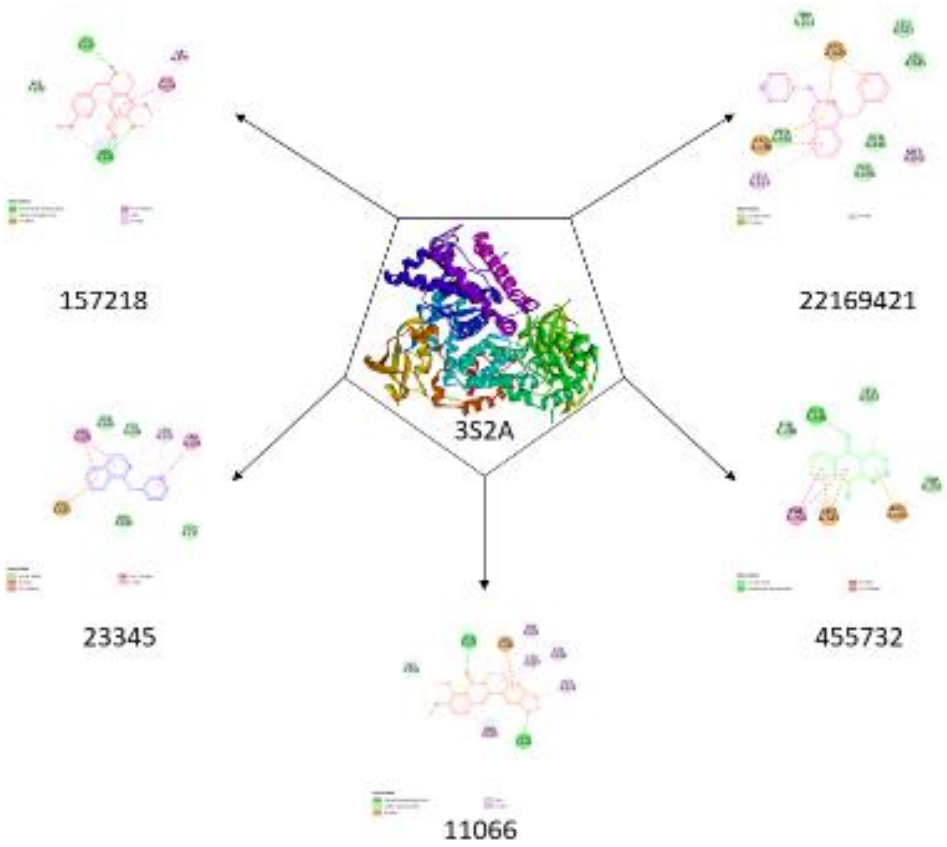

Figure 9. 2D interaction of molecular interactions of 3S2A with the ligands.

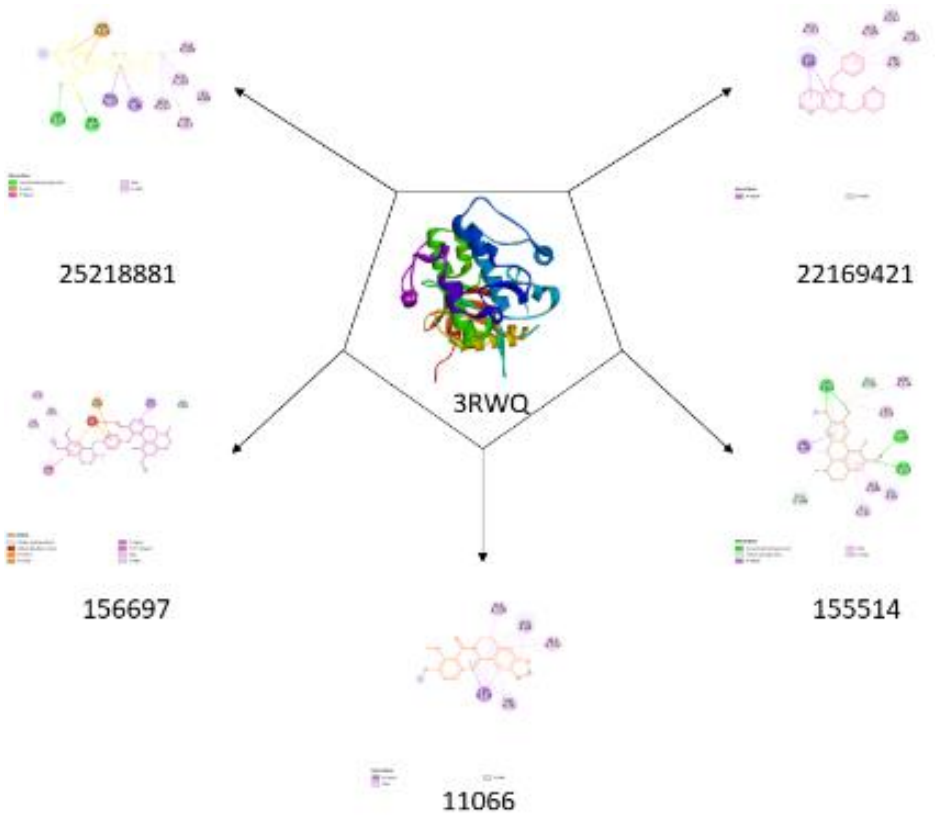

Figure 10. 2D interaction of molecular interactions of 3RWQ with the ligands.

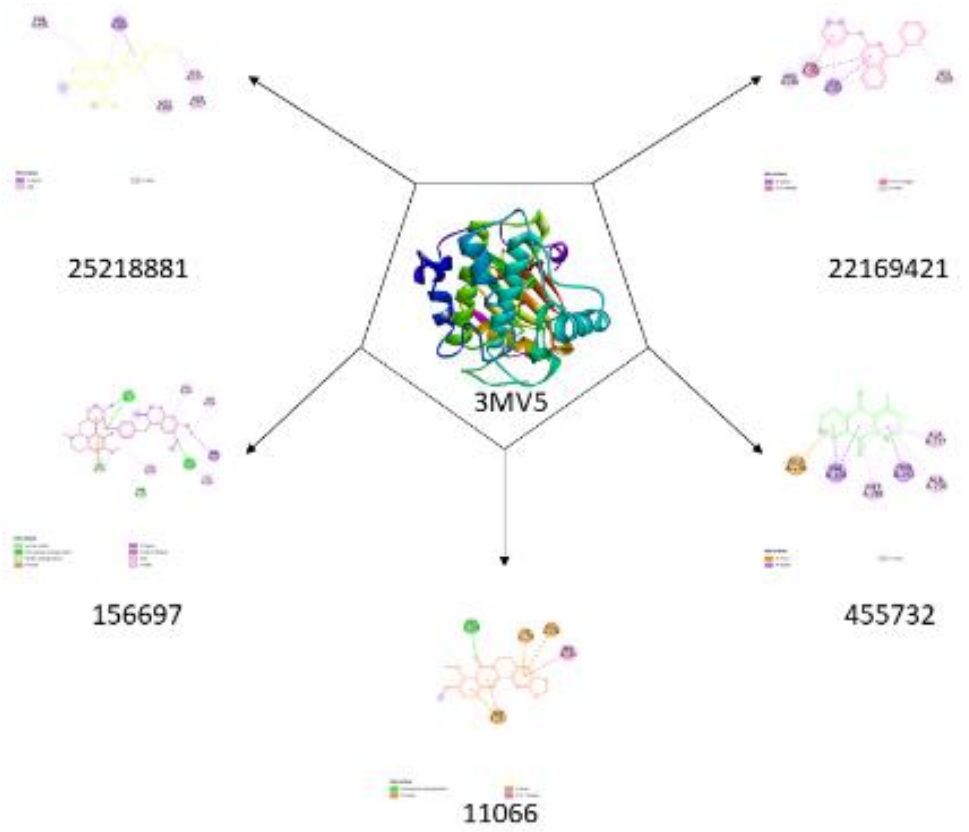

Figure 11. 2D interaction of molecular interactions of 3MV5 with the ligands.

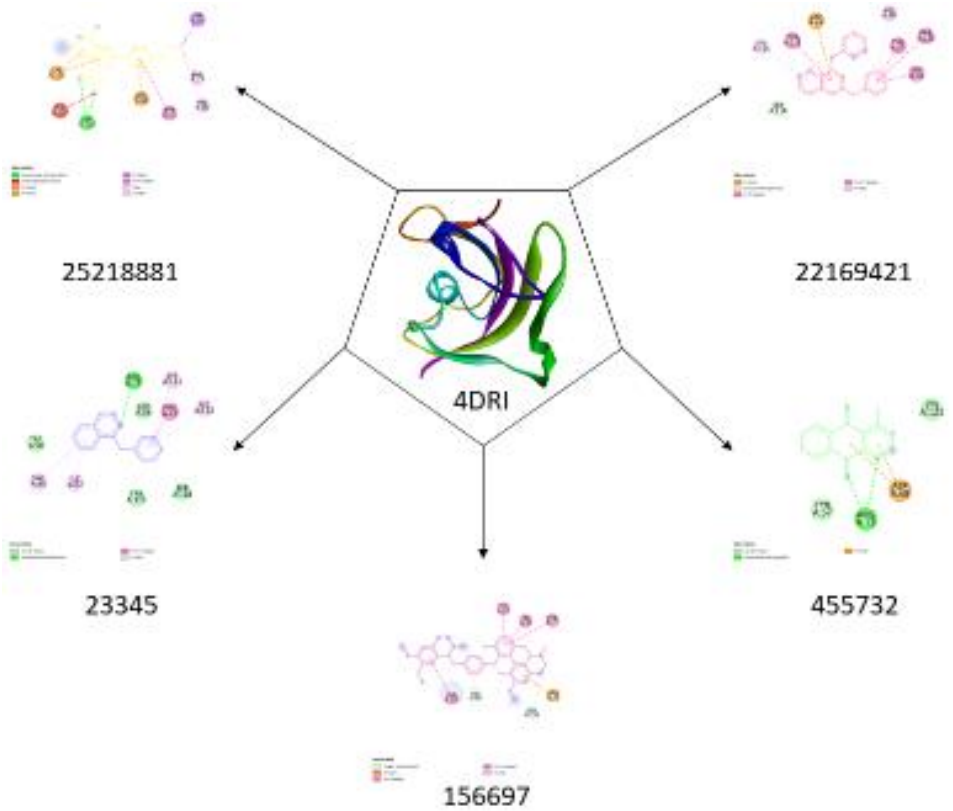

Figure 12. 2D interaction of molecular interactions of 4DRI with the ligands.

In protein 3RWQ, alkyl, Pi-alkyl, Pi-anion, and Pi-sigma were observed while binding with ligand 25218881. With ligand 22169421, Pi-sigma, and Pi-alkyl were observed. Pi-sigma, Pi-Pi T-shaped, Pi-cation, alkyl, Pi-anion, and Pi-alkyl were observed while binding with 156697. While binding with 155514, alkyl, Pi-alkyl, and Pi-sigma were observed. With 11066, Pi-sigma, Pi-alkyl, and alkyl bonds were observed (Figure 9).

In protein 3S2A, Van der Waals, Pi-alkyl, and Pi-cation bonds were observed while binding with 22169421. Binding with 457732 showed Van der Waals, Pi-cation, and Pi-Pi Stacked bonds were seen. While binding with 157218, Pi-Pi Stacked, alkyl, Pi-cation, and Pi-alkyl bonds were seen. 23345 showed Van der Waals, Pi-Pi T-Shaped, Pi-cation, Pi-alkyl, and Pi-Pi Stacked bonds were visible. While binding with 11066, alkyl, Pi-alkyl, and Pi-cation bonds were seen (Figure 8).

In protein 4DRI, Pi-sigma, Pi-Pi Stacked, Pi-cation, alkyl, Pi-anion, and Pi-alkyl bonds were visible while binding with 25218881. Binding with 22169421 showed Pi-anion, Pi-Pi T-Shaped, Pi-alkyl, Pi-Pi Stacked bonds. 457732 showed Van der Waals, Pi-anion bonds while binding. Binding with Pi-cation, Pi-Pi T-Shaped, Pi-cation, Pi-alkyl, and Pi-Pi Stacked bonds were visible while bonding with 156697. 23345 showed Van der Waals, Pi-Pi T-Shaped, and Pi-alkyl bonds were seen (Figure 7).

DISCUSSION

Targeted drug design has emerged as the most important method for drug discovery during the past few decades. Nonetheless, as multiple sites may need to be targeted at once in many multivariable and complicated disorders like cancer and diabetes, targeting single sites did not work in such cases [3]. Cell proliferation, survival, invasion, migration, apoptosis, glucose metabolism, and DNA repair are all regulated by the phosphatidylinositol 3-kinase (PI3K), protein kinase B (AKT), and mammalian target of rapamycin (mTOR) signaling pathway [16].

Quinoline is significant in medicinal chemistry since it contains a nitrogen atom, which draws electrons via resonance. This bicyclic aromatic molecule has poor tertiary base properties and is an electron-deficient system. It exhibits nucleophilic and electrophilic substitutions, while pyridine also demonstrates similar substitutions [6]. Over the years, consistent efforts have been made to create novel constituents with improved biological activity and less chance of negative side effects [1].

Recent developments in the investigation of quinoline and its relationship to cancer have revealed quinoline's potential for anticancer properties, cytotoxicity, and level of clinical treatments, which could lay the groundwork for research to develop more powerful quinoline-derived anticancer drugs [5].

Although PI3K was first discovered to bind to oncogenes and activated RTKs two decades ago, it was not until the late 1990s that it was demonstrated that the tumor suppressor PTEN acts as a phosphatase that is particular for the lipid products of PI3K that its association with human cancer was established. The relevance of the PI3K pathway in cancer has been highlighted by the discovery that numerous PI3K pathway components are commonly mutated or changed in prevalent human cancers [17].

One of the most significant intracellular pathways and a potential master regulator of cancer is phosphoinositide 3-kinase (PI3K)/activated protein kinase (AKT)/mammalian target of rapamycin (mTOR) signaling. The development of medications that target PI3K signaling has received enormous attention; several of these drugs are currently being tested in clinical trials, and it is becoming increasingly obvious that PI3K inhibitors are successful at slowing the growth of tumors [18].

In this study, possible multitarget suppression of the PI3K signaling pathway was first investigated using molecular docking modeling approaches.

Akt PBD 3MV5, PDKI 3RWQ, PIK3 3S2A, and mTOR-4DRI were chosen as the PI3K signaling components in the current investigation. The secondary structures of each were analyzed using PDBsum. 20 quinoline compounds were chosen as ligands with the help of IMPPAT. To bind ligands to protein molecules, the PyRx program was used. Phytochemicals with a binding affinity above -7 for each target protein were chosen for the docking conformation with the highest binding affinity. Then, the five ligands from each protein were chosen for further examination. The compounds 156697, 11066, 22169421, 155514, 25218881, 457732, 23345, and 157218 produced outstanding dock scores with the proteins determined with the use of docking-free energy, according to this study. They have much superior energy scores than previously reported PI3K pathway inhibitors, according to an analysis of the best docking poses of various compounds. The pharmacokinetic and pharmacodynamic characteristics of natural compounds 156697, 11066, 22169421, 155514, 25218881, 457732, 23345, and 157218 were evaluated using ADMETlab 2.0. Lipinski's Rule of Five is most effectively satisfied by the outstanding log P, molar mass, nHA, and nHD values of the ligands. The best docking-free energy score against PI3K is achieved by these substances. Their diverse pharmacodynamic and pharmacokinetic properties, many of which follow "Lipinski's Rule of Five," are what makes them notable.

CONCLUSION

There are at least eight compounds with much higher energy scores according to an analysis of the best docking poses of various chemicals. These substances have the highest docking-free energy value against PI3K. All these bioactive compounds, ligands 156697, 11066, 22169421, 155514, 25218881, 457732, 23345, and 157218 could be regarded as worthy candidates for the inhibition of the phosphoinositide-3-kinase pathway due to their high affinity for the proteins 3MV5 (Akt PBD 3MV5), 3RWQ (PDKI 3RWQ), 3S2A (PIK3 3S2A) and 4DRI (mTOR-4DRI).

Acknowledgment

I would like to thank Ms. Susha Dinesh for her guidance in undertaking the current project. I thank BioNome (*https://bionome.in/*) for offering computational facilities and help in scientific research services.

REFERENCES

1. Popova NV, Jücker M. The role of mTOR signaling as a therapeutic target in cancer. Int J Mol Sci. 2021;22(4):1743. doi: 10.3390/ijms22041743.
2. Mishra R, Patel H, Alanazi S, Kilroy MK, Garrett JT. PI3K inhibitors in cancer: clinical implications and adverse effects. Int J Mol Sci. 2021;22(7):3464. doi: 10.3390/ijms22073464.
3. Singh P, Bast F. Multitargeted molecular docking study of plant-derived natural products on phosphoinositide-3 kinase pathway components. Med Chem Res. 2014;23(4):1690–700. doi: 10.1007/s00044–013–0774–2.
4. Cantley LC. The phosphoinositide 3-kinase pathway. Science. 2002;296(5573):1655–7. doi: 10.1126/science.296.5573.1655.
5. Ilakiyalakshmi M, Arumugam Napoleon AA. Review on recent development of quinoline for anticancer activities. Arab J Chem. 2022;15(11):104168. doi: 10.1016/j.arabjc.2022.104168.
6. Ma X, Shen L, Zhang J, Liu G, Zhan S, Ding B et al. Novel 4-acrylamido-quinoline derivatives as potent PI3K/mTOR dual inhibitors: the design, synthesis, and in vitro and in vivo biological evaluation. Front Chem. 2019;7:236. doi: 10.3389/fchem.2019.00236.
7. Moor LFE, Vasconcelos TRA, da R Reis R, Pinto LSS, da Costa TM. Quinoline: an attractive scaffold in drug design. Mini Rev Med Chem. 2021;21(16):2209–26. doi: 10.2174/1389557521666210210155908.
8. Jain S, Chandra V, Kumar Jain PK, Pathak K, Pathak D, Vaidya A. Comprehensive review on current developments of quinoline-based anticancer agents. Arab J Chem. 2019;12(8):4920–46. doi: 10.1016/j.arabjc.2016.10.009.
9. Mohanraj K, Karthikeyan BS, Vivek-Ananth RP, Chand RPB, Aparna SR, Mangalapandi P et al. IMPPAT: A curated database of Indian Medicinal Plants, Phytochemistry and Therapeutics. Sci

Rep. 2018;8(1):4329. doi: 10.1038/s41598–018–22631-z.
10. Kim S, Chen J, Cheng T, Gindulyte A, He J, He S et al. PubChem in 2021: new data content and improved web interfaces. Nucleic Acids Res. 2021;49(D1):D1388–95. doi: 10.1093/nar/gkaa971.
11. Burley SK, Berman HM, Kleywegt GJ, Markley JL, Nakamura H, Velankar S. Protein Data Bank (PDB): the single global macromolecular structure archive. Methods Mol Biol. 2017;1607:627–41. doi: 10.1007/978–1–4939–7000–1_26.
12. Kemmish H, Fasnacht M, Yan L. Fully automated antibody structure prediction using BIOVIA tools: validation study. PLOS ONE. 2017;12(5):e0177923. doi: 10.1371/journal.pone.0177923.
13. de Beer TA, Berka K, Thornton JM, Laskowski RA. PDBsum additions. Nucleic Acids Res. 2014;42((Database issue)):D292–6. doi: 10.1093/nar/gkt940.
14. Dallakyan S, Olson AJ. Small-molecule library screening by docking with PyRx. Methods Mol Biol. 2015;1263:243–50. doi: 10.1007/978–1–4939–2269–7_19.
15. Xiong G, Wu Z, Yi J, Fu L, Yang Z, Hsieh C et al. ADMETlab 2.0: an integrated online platform for accurate and comprehensive predictions of ADMET properties. Nucleic Acids Res. 2021;49(W1):W5-W14. doi: 10.1093/nar/gkab255.
16. Miricescu D, Totan A, Stanescu-Spinu II, Badoiu SC, Stefani C, Greabu M. PI3K/AKT/mTOR signaling pathway in breast cancer: from molecular landscape to clinical aspects. Int J Mol Sci. 2020;22(1):173. doi: 10.3390/ijms22010173.
17. Liu P, Cheng H, Roberts TM, Zhao JJ. Targeting the phosphoinositide 3-kinase pathway in cancer. Nat Rev Drug Discov. 2009;8(8):627–44. doi: 10.1038/nrd2926.
18. Yang J, Nie J, Ma X, Wei Y, Peng Y, Wei X. Targeting PI3K in cancer: mechanisms and advances in clinical trials. Mol Cancer. 2019;18(1):26. doi: 10.1186/s12943–019–0954-x.

